



Optimizing the Plasmonic Sensing of Silica Coated Au/Ag Nanoshells

Hafiz Zeeshan Mahmood¹, Sajid Farooq², Emery C. Lins³

^{1,3}Federal University of Pernambuco, Recife, Brazil

²University of Pernambuco, Recife, PE, Brazil

(¹hafiz.mahmood@ufpe.br, ²sajiddahar@gmail.com, ³emerylins@gmail.com)

Abstract- The plasmonic sensing performance is governed by the bulk sensitivity and the line width of the localized surface plasmon resonance (LSPR) peak. Therefore, a sensor requires addressing formention above parameters: a good bulk sensitivity (RIS) and sharp LSPR spectrum, correlated by RIS×FoM. Complex plasmonic nanostructures are proposed for sensing applications due to their high sensing ability without considering the broad nature of the LSPR peak that decrease the detection limit of the plasmonic sensor. In this article, we applied Full-wave field analysis/Mie theory to compute the optical characteristics and exploring the potential of dielectric shell with metallic core (Au/Ag@SiO₂) under probe model as a reliable sensor. On tuning the geometric parameters of the nan shells, we have calculated the optimized RIS×FoM parameter with a value of 479 nm/RIU₂ for Ag@SiO₂ whereas for Au@SiO₂ is 364 nm/RIU₂. Furthermore, Campbell's model was exploited for molecular adsorption sensing on a size dependence approach. These finding poses that our proposed multilayer geometry can be extended to other systems by enabling the plasmonic sensors to have a better efficacy over wide spectral ranges with high accuracy and good stability.

Keywords- Localized Surface Plasmon Resonance, Bulk Sensitivity (RIS), Figure Of Merit (FoM)

I. INTRODUCTION

Over the last two decades extensive efforts has been exerted to explore the impact of the geometry and composition of nanoparticles (NPs) on its optical properties [1-3]. An interesting phenomenon provokes when light interacts with noble metals nanostructures designated as Localized Surface Plasmon Resonance (LSPR), i.e. the collective oscillations of the conduction electrons (Non- Propagating) prompted by electromagnetic radiation having a specific wavelength.

A plethora of studies showed that LSPR wavelength of the nanoparticles is directly linked to the shape, size and metal composition which make them pragmatic for the optical phenomenon (absorption, scattering, extinction) of light and bio sensing [4-8]. Due to their unique optical properties and multifaceted approach, plasmonic nanostructures persistently

utilized in the area of biological sensing and chemical detection [9-12]. To foster the sensitivity, phenomenon of sensing utilizes the capability of metallic nanostructures to concentrate the external radiation in the vicinity of their small local entity. It has been studied that Refractive index (RI) based sensitivity and figure of merit, (defined as the ratio of sensitivity to the line width), depends on the geometry of the Au nanoparticles [13, 14]. For single particle LSPR sensor, the fundamental principle utilizes the fact that LSPR spectrum position varies as a function of dielectric host medium [7]. Jensen and Mock et al [15-16] pointed out that LSPR wavelength of metallic nanoparticles shift with respect to variation in the RI of the proximity of surrounding media.

To investigate which metal nanostructures is a good candidate for bio or chemical sensing applications as well as their efficiency can be characterized by measuring RI based sensitivity. In order to correlate the varying RI of the surrounding medium and peak shift of the LSPR wavelength that governs the sensing performance of LSPR sensor, an important sensing parameter to analyze the sensing efficiency has been evaluated qualitatively i.e. Bulk sensitivity: $\eta b = \Delta\lambda_{LSPR} / \Delta n$, where $\Delta\lambda_{LSPR}$ is change in LSPR wavelength as function of change in refractive index of the surrounding medium (Δn).

Second parameter to analytically describe the sensor reliability is the Figure of Merit, $FoM = \eta b / FWHM$, where (FWHM) is full width at half maximum or line width of the LSPR peak. Therefore, a LSPR sensor requires attending simultaneously both prerequisites: high bulk sensitivity and a fine LSPR spectrum. This condition can be depicted by a relation given as RIS×FoM

Furthermore, Au/Ag Nano shell based on gold/silver core encapsulated by silica shell having Nano scale varying thickness likewise their tune ability linked with surface plasmon resonance were also theoretically investigated. The simulations were carried out by Finite Element Method (FEM) based on partial differential equations by commercially available software COMSOL Multiphysics 5.1, which is an efficient tool to explore the electromagnetic properties as well as their electric field distribution on the surface of nanostructures having various shapes to predict the unprecedented dependence of the plasmonic properties of core-

shell Nano scale structure [17]. To determine the scattered field distribution and extinction cross section, the Nano aggregates surface was divided into extremely small mesh elements up to finer size. The amplitude was fixed 1 Vm⁻¹ for background field oscillations. A hindrance was created in shape of perfectly matched layer around the nanostructure to limit the simulation from any reflection.

II. MODELLING AND CALCULATIONS

Fig. 1 illustrates the schematic geometry of Au/Ag silica coated Nano shell being studied in this work. The inner most region is attributed as core having radius and dielectric function r_1 and ϵ respectively. The second portion represents the shell with radius r_2 and dielectric function ϵ_d , where shell thickness is given by $t = r_2 - r_1$.

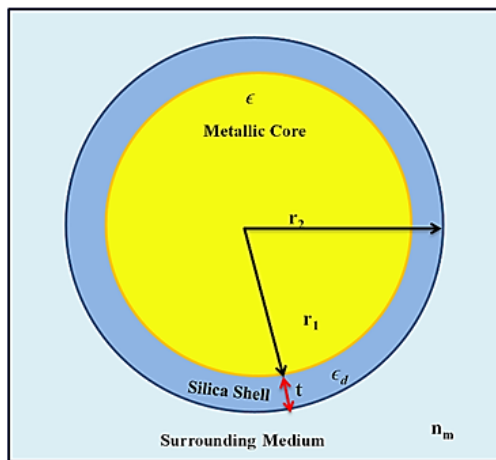


Figure 1. Schematic model of the metallic core with dielectric (SiO_2) coated nanoshell.

The interaction between core-shell based metallic nanostructures and electromagnetic radiation in this study was ascribed by Mie theory which elucidated well the solution of Maxwell's equation with appropriate boundary conditions.

Let N be the number of particles per unit volume were contained in a dilute colloidal solution illuminated by incident light, the measured attenuation in the intensity of light I_0 , for a path length l_d in cm is given by [18].

$$M_a = \log \frac{I_0}{I_d} = NC_{ext} \left(\frac{d}{2.303} \right) \quad (1)$$

Where C_{ext} is extinction cross section which can be calculated by the following relation given by [19].

$$C_{ext} = \frac{2\pi}{k^2} \sum (2n+1) R_e (a_n + b_n) \quad (2)$$

where R is the radius and k are the wave number in the surrounding medium, a_n and b_n are scattering coefficients as well as the function of radius. To determine the position of LSPR extinction spectra, The extinction cross section (C_{ext}) can be estimated after figuring out the values of (σ_{abs}) and (σ_{sca}). From Mie theory the values for absorption and scattering can be calculated as [20]:

$$\sigma_{abs} = \frac{2\pi}{\lambda\epsilon_0} \text{Im}(\alpha) \quad \text{and} \quad \sigma_{sca} = \frac{8\pi^3}{3\lambda^4\epsilon_0^2} |\alpha|^2 \quad (3)$$

It is obvious from (3), both are functions of ϵ_0 and λ , therefore it is quite feasible to plot the σ_{ext} in order to get the position of Plasmon peak. In this study the silica thickness and the diameter of the core both are variable i.e. the dielectric function is size-dependent. When the dielectric function is geometrically tunable, the effect of electron scattering can be interpreted by practicing the modified bulk collision frequency:

$$\Gamma = \Gamma_{bulk} + \frac{Av_f}{m_f} \quad (4)$$

where Γ_{bulk} , m_f and v_f are collision bulk frequency, electron mean free path and Fermi velocity respectively. In case of single refractive scattering and for simple Drude model, $A = 1$ [18]. But customarily its value lies in between 1-5 [19]. Whereas, A is a dimensionless geometrical parameter. For Nano shells, the bulk dielectric function can be modified to analyze the free electrons scattering, which is given by:

$$\epsilon(m_f, \omega) = \left(1 - \frac{\omega_{bp}^2}{\omega^2 + i\omega\Gamma} \right) + \epsilon(\omega)_{int} \quad (5)$$

Here, the second term represents the interband transitions, ω_{bp} bulk plasma frequency, m_f mean free path of reduced electrons and $\epsilon(m_f, \omega)$ is metallic dielectric function (size dependent).

III. RESULTS AND DISCUSSION

In this probed model, our focus is on the optimization of the figure of merit by varying the refractive index of the surrounding medium. Despite their simplest core-shell based structure, these metallic nanostructures can still display refractive index tunability based on their LSPR effect. Fig. 2 (A & B) depicted the response of the λ_{LSPR} and extinction spectra of metallic core/dielectric shell nanoparticles to the refractive index of the neighboring medium respectively. For both nanostructures, by varying the RI the extinction varied significantly in the visible regime and exhibits red shifts which obviously results increase in the intensity of the extinction peak.

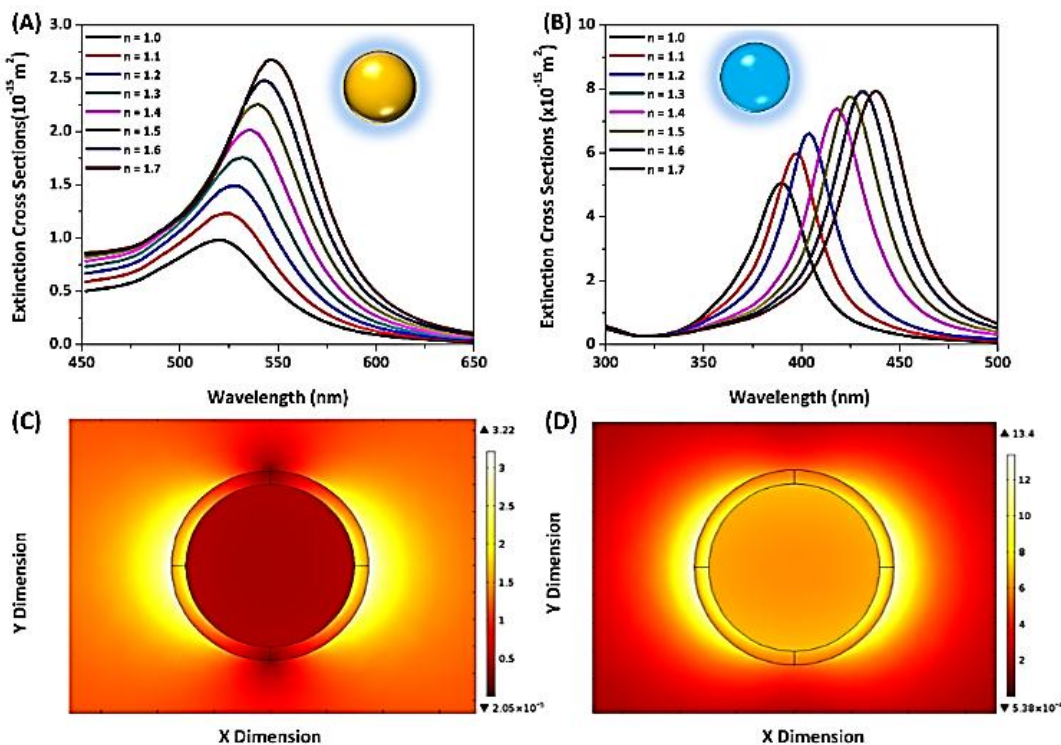


Figure 2. The LSPR extinction for gold (A) and silver (B) nanoshells. Electric field profile for gold (C) and silver nanoshells (D) in dielectric media water.

In case of Au@SiO₂ shell, the extinction spectra continued to red shift in the visible region and the peak wavelength approaches 540 nm. On contrary, the extinction peak of Ag@SiO₂ shell initially blue shifted near UV regime and eventually the peak wavelength was recognizable around 430 nm in the visible region. The E-field profile around the Nano shells for the dipole mode (gold and silver) can be observed in Fig. 2C-D respectively. The changes in normalized electric field of Nano shells were compared at the LSPR wavelengths. For linear polarization, the electric field distribution is expressed by the two lobes which ensure the influence of plasmon dipole resonance. LSPR peak position can be determined not only by the real part of nanostructure dielectric function, but also by the RI of the surrounding medium. In refractive index based LSPR sensors, bulk sensitivity reflects how LSPR peak position varies by changes in the RI of the local medium. Fig. 3 depicts that surface plasmon wavelength as a function of RI which increases linearly along with refractive index range from 1.0 to 1.5 for both (Au/Ag) plasmonic nanostructures. In case of Ag@SiO₂ nanoparticles with radius of 30 nm, ($t = 5 \text{ nm}$), there is red-shift effect from 390 to 424 nm ($\Delta\lambda \approx 27 \text{ nm}$), as observed in Fig. 3. On the other hand, for the Au@SiO₂, the plasmonic shift influence is around $\Delta\lambda \approx 20 \text{ nm}$ (Fig. 3), indicating that Ag Nano shells show more sensitivity to surrounding environment. Moreover, one can see that the plasmon peak shift is linearly reliant on the RI of dielectric surrounding media.

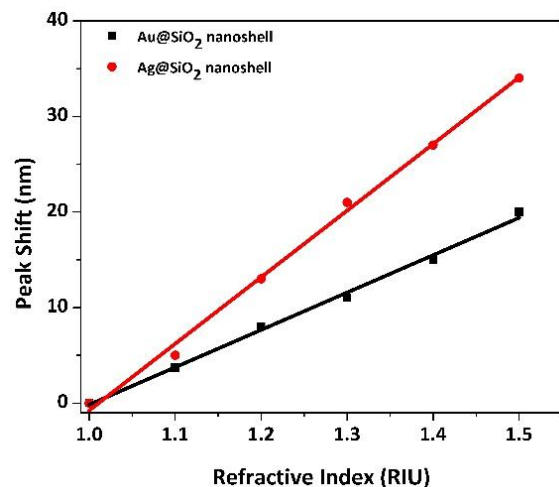


Figure 3. LSPR peak shift of gold and silver nanoshells on changing the refractive index of the surrounding medium.

Fig.4 reflects the sensitivity response of the plasmonic sensor when R_c thickness of Ag and Au is fixed (30 nm) while SiO₂ shell radius is tuned from 2 to 18 nm. As expected, increasing the shell thickness results in decreasing the sensitivity for both metallic cores, specifically linearly for Ag Nano shell. Keeping in view this response based on this proposed structure, for high molecular sensing Ag@SiO₂

nanostructure could be more useful for molecular bio sensing at small shell thickness (5 nm) as compared to Au@SiO₂ shell.

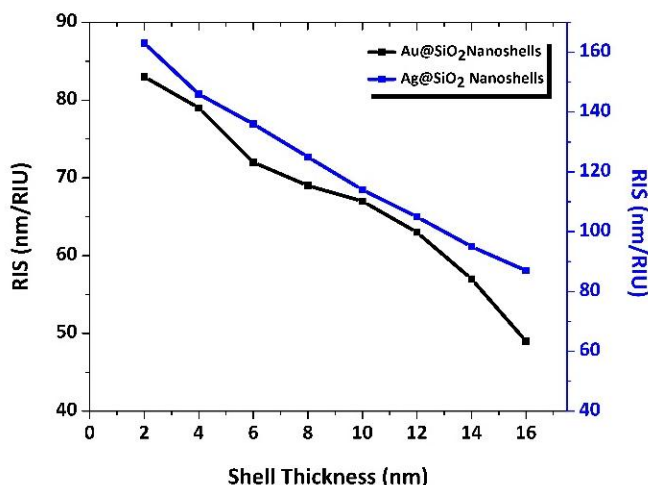


Figure 4. The sensitivity of gold and silver nanoshells as a function of their respective silica shell thickness.

The effects of NP core radius on the bulk sensitivity and FoM determining nanoparticle sensing efficiency can be observed in Fig. 5. Ag and Au Nano shells with radii 10 - 50 nm (t = 5nm) were analyzed. A theoretical analysis of the bulk

sensitivity as function of core radius Fig. 5 A indicates a linear behavior for the sensitivity values. As the core radius of the nanoparticles increases, a linear response in Nano sensor bulk sensitivity from 20-140 nm/RIU for gold, and 40 - 240 nm/RIU for silver Nano shells were respectively observed.

As core shell radius increases, the sensing area as a function of radius of the core shell linearly increases, results in raising the sensitivity of the nanostructured platform. Moreover, for small particle ($r < 10$ nm) the absorption process mainly determines the light nanoparticle interaction. Scattering phenomenon enhance by increasing the particle size ($r > 10$ nm). In case of AuNP platform, with $20 \text{ nm} < r < 40 \text{ nm}$ bulk sensitivity is highly dependent on the nanostructure size. It can be seen (Figure 5) that bulk sensitivity of Ag Nano shells is highly influenced on size than Au Nano shells. As the Ag Nano shell radius increases, the FWHM increase due to radiation damping factor [21]. Therefore, FoM of Ag Nano shells decrease as the particle size grows, as shown in Fig. 4(B). Albeit, the ϵ_i value of Ag dielectric function is less than that of Au across visible region, therefore less damping occurs, resulting narrow FWHM in previous section (Fig. 2) and high values of FoM for in previous section (Fig. 2) and high values of FoM for silver particles. This is an advantage of Ag over Au Nano shells in bio sensing applications. The calculated value of FoM (3.0) depicted in Fig. 5(B) for silver Nano shells ($r = 30$ nm) is higher than the reported values of more complex shapes, such as single Au Nano rod (1.3) [22], Au Nano star (1.9) [23], Au pyramid (2.2) [24] Ag Nano cube (1.6) [25].

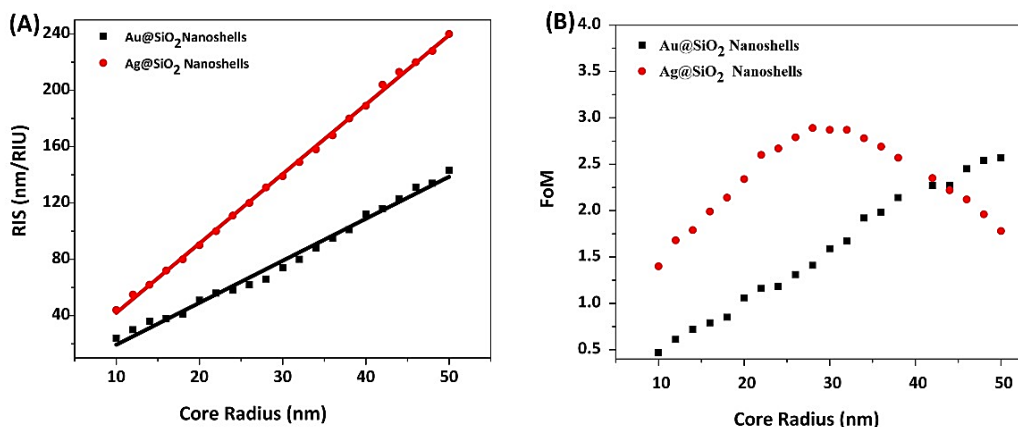


Figure 5. (A) The bulk sensitivity of gold versus silver nanoshells as a function of core radius (B) and their respective figure of merit.

The FWHM of gold spectrum is not so affected by changing the surrounding medium, as compared to Ag Nano platform. Therefore, the FoM response of AuNP is mainly determined by variations in bulk sensitivity. Furthermore, the relation RIS× FoM provides an over view of the sensing ability of LSPR sensor. Figure 6 depicts the RIS× FoM values for Au/Ag@SiO₂ Nano shell with different core radius, ranging from 10 to 50nm (shell thickness 5nm), indicating that R_c=30nm provides the best performance for the LSPR sensor at t = 5nm, where RIS×FoM is equal to 479 nm/RIU² for Ag as compare to Au Nano shells (364nm/RIU²).

On optical based bio sensing, the EM field decay length (l_d) is considered an important parameter for molecular sensing [26].

Due to a molecular monolayer adsorption, the LSPR wavelength shift ($\Delta\lambda$) on a metallic NP surface can be ascribed by the Campbell's model as:

$$\Delta\lambda = \eta_b(n_{ads} - n_m)(1 - e^{-2d/l_d}) \quad (6)$$

The Campbell's model (Eq. 6) indicates the $\Delta\lambda$ decreases as the l_d value increases. Where l_d is the EM field decay length

around the NP, adsorbate layer thickness d , η_b is the bulk sensitivity and n_{ads} , n_m are respectively the RI of the adsorbate layer and the surrounding dielectric medium [26].

In Bio sensing, the adsorption of a molecular layer on a metallic NP surface enhances shifts in the LSPR spectrum according to the Campbell's model. Fig. 7 shows the trend of LSPR peak shift of the plasmonic Nano shells when the monolayer thickness (d) with RI (1.48) equal to protein on the NP surface is observed ($d = 0.5$ to 10 nm). For a 10 nm thick monolayer, a red-shift effect of $\Delta\lambda \approx 65.90$ nm for Ag@SiO₂ and $\Delta\lambda \approx 50.10$ nm in case of Au@SiO₂ respectively can be observed. However, Fig. 7 demonstrates that Ag@SiO₂ is more sensitive to adsorbed layer as compared to Au@SiO₂ Nano shells (50 nm radius).

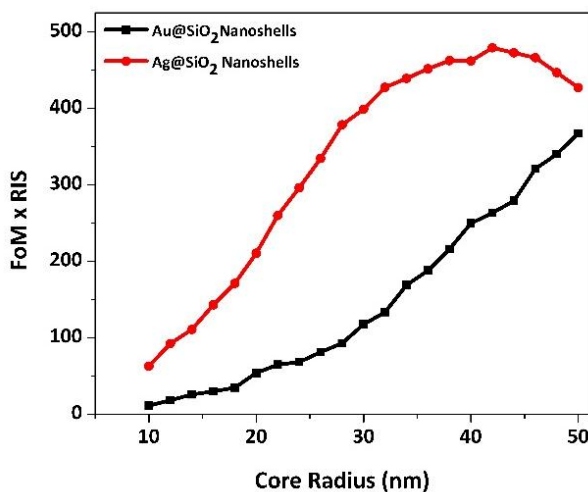


Figure 6. The product of RIS×FoM (unit: nm/RIU²) for Au/Ag nanoshell with SiO₂ shell (5nm) and Au/Ag core (10-50nm).

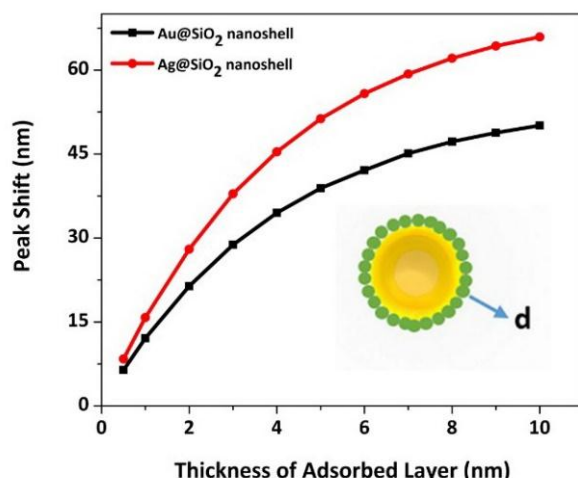


Figure 7. Plasmonic spectral shift as a function of the adsorbent layer thickness (d) with a refractive index of $n_d=1.48$; for Au/Ag core $R_c = 30$ nm ($t=5$ nm) nanoshells employing Campbells model.

IV. CONCLUSION

The sensing performance of the metallic core (Au/Ag) with SiO₂ shell nanostructure is investigated, regarding the RIS×FoM relation that ascribes the sensing performance given by the product of the high bulk sensitivity and a sharp LSPR spectrum of a sensor. We have calculated an optimized performance of this probed LSPR sensor by applying RIS×FoM parameter with a value of 479 nm/RIU² for Ag on contrary for Au is 364 nm/RIU² respectively.

The Campbell's model indicated a higher LSPR spectrum shift ($\Delta\lambda \approx 65.90$ nm) due to the adsorption of a 10nm thick molecular layer on the Ag@SiO₂, which is higher than Au@SiO₂ Nano shell ($\Delta\lambda \approx 50.10$ nm). Besides, the optimizing approached used in this work can be extended to different nanostructures, establishing a new paradigm on engineering LSPR biosensor.

ACKNOWLEDGMENT

The authors thank the support of National Council for Scientific and Technological Development (CNPq) and H Zeeshan Mahmood PhD student, is grateful to CAPES (Brazil) for the financial support during this work

REFERENCES

- [1] Sherry LJ, Chang SH, Schatz GC, Van Duyne RP, Wiley BJ, Xia Y, Localized surface plasmon resonance spectroscopy of single silver nanocubes. *Nano letters*. 2005, 5(10):2034–2038.
- [2] Chen H, Kou X, Yang Z, Ni W, Wang J, Shape-and size-dependent refractive index sensitivity of gold nanoparticles. *Langmuir*. 2008, 24(10):5233–5237.
- [3] Murray WA, Auguié B, Barnes WL, Sensitivity of localized surface plasmon resonances to bulk and local changes in the optical environment. *The Journal of Physical Chemistry C* 2009, 113(13):5120–5125.
- [4] Petryayeva E, Krulle UJ: Localized surface plasmon resonance: Nanostructures, bioassays and biosensing—A review. *Analytica Chimica Acta* 2011, 706: 8–24.
- [5] K.S. Lee, M.A. El-Sayed, Gold and silver nanoparticles in sensing and imaging: Sensitivity of plasmon response to size, shape, and metal composition, *J. Phys. Chem.* 2006, B 110: 19220–19225.
- [6] Farooq S, Neves WW, Pandoli O, Del Rosso T, de Lima LM, Dutra RF, de Araujo RE. Engineering a plasmonic sensing platform for italic candida albicans/italic antigen identification. *J Nanophotonics*, 2018,12(3):033,003
- [7] Ribeiro MS, de Melo LS, Farooq S, Baptista A, Kato IT, N' unez ~SC, de Araujo RE. Photodynamic inactivation assisted by localized surface plasmon resonance of silver nanoparticles: in vitro evaluation on escherichia coli and streptococcus mutans. *Photodiagn Photodyn Ther* 2018, 22:191–196
- [8] H.X. Xu, M. Käll, Modeling the optical response of nanoparticle-based surface plasmon resonance sensors. *Sens. Actuators B* 87 2002, 244–249.
- [9] A. Pranzetti, S. Salatiñ, S. Mieszkin, M.E. Callow, J.A. Callow, J.A. Preece, P.M. Mendes, Model organic surfaces to probe marine bacterial adhesion kinetics by surface plasmon resonance, *Adv. Funct. Mater.* 22 2012, 3672–3681.
- [10] T. Chen, M.X. Xin, X.J. Wang, L.H. Tan, H.Y. Chen, Controlled assembly of eccentrically encapsulated gold nanoparticles, *J. Am. Chem. Soc.* 130 2008, 11858–11859.

- [11] S. Lal, S. Link, N.J. Halas, Nano-optics from sensing to waveguiding, *Nat. Phot.* 1 2007, 641–648.
- [12] J. Cao, T. Sun, M.H. Tu, K.T.V. Grattan, Wavelength-based localized surface plasmon resonance optical fiber biosensor, *Sens. Actuators B Chem.* 181 2013, 611–619.
- [13] Klantsataya, E. A. François, H. Ebendorff-Heidepriem , P. Hoffmann and T. M. Monro, Surface Plasmon Scattering in Exposed Core Optical Fiber for Enhanced Resolution Refractive Index Sensing, *Sensors.* 15 2015, 25090-25102.
- [14] C. Huanjun, X. Kou, Z Yang, W. Ni, J. Wang: Shape and size dependent Refractive index sensitivity of Gold Nanoparticles, *Langmuir.* 24 2008, 5233-5237.
- [15] T.R. Jensen, M.L. Duval, K.L. Kelly, A.A. Lazarides, G.C. Schatz, R.P. Van Duyne, Nanosphere lithography: effect of the external dielectric medium on the surface plasmon resonance spectrum of a periodic array of silver nanoparticles, *J. Phys. Chem. B* 103 1999, 9846–9853.
- [16] J.J. Mock, D.R. Smith, S. Schultz, Local refractive index dependence of plasmon resonance spectra from individual nanoparticles, *Nano Lett.* 3 2003, 485–491.
- [17] Du, C. M. Huang, T. Chen, F. Sun, B. Wang, C. He and D. Shi. Linear or quadratic plasmon peak sensitivities for individual Au/Ag nanosphere sensors, *Sens. Actuators B Chem.* 203 2014, 812–816.
- [18] Averitt, R. D., S.L. Westcott and N.J. Halas. Linear optical properties of gold nanoshells. *J optical society of America B.* 16, 1999, 1824-1832.
- [19] C.F. Bohren, D.R. Huffman, *Absorption and Scattering of Light by Small Particles*, Wiley, New York, NY, 1983.
- [20] Ishimaru , A. *Wave Propagation and Scattering in Random Media*, Academic Press , New York, 1978.
- [21] Hu, H., Novo, C., Funston, A., Wang, H., Staleva, H., Zou, S., Mulvaney, V., Xiae, Y. and Hartland, G.V. Dark-Field Microscopy Studies of Single Metal Nanoparticles: Understanding the Factors That Influence the Line Width of the Localized Surface Plasmon Resonance. *Journal of Materials Chemistry*, 18, 2008,1949-1960.
- [22] Mayer, K.M., Lee, S., Liao, H., Rostro, B.C., Fuentes, A., Scully, P.T., Nehl, C.L. and Hafner, J.H. A Label-Free Immunoassay Based upon Localized Surface Plasmon Resonance of Gold Nanorods. *ACS Nano*, 2, 2008, 687-692.
- [23] Nehl, C.L., Liao, H. and Hafner, J.H. Optical Properties of Star-Shaped Gold Nanoparticles. *Nano Letters*, 6, 2006, 683-688.
- [24] Lee, J., Hasan, W. and Odom, T.W. Tuning the Thickness and Orientation of Single au Pyramids for Improved Refractive Index Sensitivities. *The Journal of Physical Chemistry C*, 113 ,2009, 2205-2207.
- [25] Sherry, L.J., Chang, S.H., Schatz, G.C., Van Duyne, R.P., Wiley, B.J. and Xia, Y. Localized Surface Plasmon Resonance Spectroscopy of Single Silver Nanocubes. *Nano Letters* , 5, 2005, 2034-2038.
- [26] Farooq S, Rativa D , de Araujo. Optimizing the Sensing Performance of SiO₂-Au Nanoshells. *Plasmonic*, pp 1-8, 2019.

How to Cite this Article:

Mahmood, H. Z., Farooq, S. & Lins, E. C. (2019) Optimizing the Plasmonic Sensing of Silica Coated Au/Ag Nanoshells. *International Journal of Science and Engineering Investigations (IJSEI)*, 8(87), 140-145. <http://www.ijsei.com/papers/ijsei-88719-23.pdf>

